

## Characterization of the Microstructural and Mechanical Properties of MoZrN Coating

Abdelaziz Abboudi<sup>1,2\*</sup>, Brahim Chermime<sup>1,2</sup>, Hamid Djebaili<sup>2,3</sup>, Mourad Brioua<sup>1</sup>

<sup>1</sup> Department of mechanic, University Hadj Lakhdar, Batna 05000, Algeria

<sup>2</sup> Laboratoire des Sciences, Universite Abbas Laghrour, 40000 Khenchela, Algeria

<sup>3</sup> Department of Mechanic, University Abbas Laghrour, 40000 Khenchela, Algeria

(Received 23 December 2016; revised manuscript received 07 January 2017; published online 20 February 2017)

The aim of this paper is evaluation of properties of samples with The ternary nitride (Mo,Zr)N thin films were grown on silicon and steel XC100 substrates by the reactive RF magnetron sputtering technique. The substrates were exposed to ion bombardment coating, which was deposited on two types of substrates. Silicon was made by melt technology, this method belongs to PVD (Physical Vapour deposition) process. Thin PVD coatings deposited onto surface of tools and machine parts are widely used in a range of sectors, for example in machine engineering. These materials, wear resistance and thermal and chemical stability of the surface. Structure, chemical composition a properties of thin layers depend on technological parameters of the PVD process and preparation of steel substrate. High requirements on the quality of thin PVD coatings resulted in development of methods used to evaluate of their properties. The thickness is one of the important characteristics of mechanical properties of the coated parts. The surface morphology, microstructure, and composition were studied by atomic force microscopy (AFM) nanoindentation, scanning electron microscopy (SEM) and X-ray diffractometer.

**Keywords:** Microstructure, The thickness, PVD coatings, Morphology.

DOI: [10.21272/jnep.9\(1\).01014](https://doi.org/10.21272/jnep.9(1).01014)

PACS numbers: 61.72. – y, 62.20.D –

### 1. INTRODUCTION

The first cover PVD was introduced in the middle of the years eighty. Since this introduction, progress was brought to the methods of deposits PVD which allowed the obtaining of new covers with clean properties to there never reached by the conventional methods CVD [1]. Over the years, he was acquired that the application of hard covers in thin layers by various methods of deposits PVD on the tools of manufacturing improves clearly the performances of these products [2].

These hard covers present a high mechanical hardness combined(organized) in a good thermal and chemical stability. These covers give the opportunity to be able to adjust properties as the parameter of stitch, the hardness, the elasticity, the coefficient of thermal expansion or the behavior in corrosion to optimize The advantages of the thin coats(layers) developed by these methods include a high strength in the wear, a good tenacity, a chemical and thermal stability as well as a low(weak) coefficient of friction [2-3]. Nitrides of metals of transition (such as the ZrN, TiN, CrN, HfN, NbN, ZrBN, TiAlN, TiCrN, CrAlN) train(form) a very vast range of materials possessing interesting physical properties grace(favor) in which they are very used in numerous applications manufacturers cover [4-5]. The use of coatings of the nitride of transition metals has been explored with success in the past decades, due to properties such as high hardness, biocompatibility, wear and corrosion resistance and thermal stability. Titanium nitride is the most studied. However, zirconium, niobium nitrides, and vanadium, among others, also have similar protective properties [6]. Authors agree on the values of hardness of about 25 GPa for TiN [7]. In order to determine the process of forming of these films, depending on the used equipment, a strict

control of all deposition parameters is required. Currently, the technique most commonly used is the coating of metal surfaces with reactive nitrides magnetron sputtering which enables the handling of a large number of parameters such as energy deposition (bias), deposition rate (plasma current), residual stresses of the layer thickness and a neutral reagent gas showed that CrN compared to TiCN, ZrN, TiN [8]. has the wear rate is the lowest.

### 2. EXPERIMENTAL PROCEDURE

ZrN and MoZrN deposits are made ENSAM of cluny using System Dual magnetron sputtering (Nordiko 3500). was process to remove air history to create a vacuum to  $10^{-6}$  torr. There after we has set the desired polarization with Argon fixation and progressive increase of the nitrogen pressure.

XC100 was used as substrate material and polished to a surface roughness of 0.09 mm, after the polishing process, the sample was ultrasonically cleaned in hot alkaline cleaning bath for at least 5 min and then quenched. The target, composed of materials to be sprayed, are connected to a RF generator (13.56 MHz) power of a variable from 0 to 1250 W), (Fig.1) with Mo and Zr target and nitrogen gas as reagent, a substrate XC100. Sources of Zr and Mo were installed on each side of the chamber wall, the distance between the substrate and the targets was fixed around 8 cm. The variation in the percentage of Zirconium (Zr) is made by changing the voltage on the target (Zr) by setting the voltage of the Mo target, a second series of depositions were carried out by setting the voltage of the Zr target and varying the voltage e Mo target, the deposition time is 100 min .The chemical composition of the steel XC100 is given in the following table

\* [abboudiabdalaziz@yahoo.fr](mailto:abboudiabdalaziz@yahoo.fr)



**Fig. 1** – Magnetron sputtering system. '1' pumping system, '2' filing cabinet, '3' mass flowmeters, '4' pressure drive, '5' DC power supply, '6' 13.56 MHz RF generator, '7' stub, '8' quadrant control, '9' turntable motor substrate holder (PS), '10' automaton

**Table 1** – Chemical composition of XC100 steel wt. %

XC100	C	Mn	S. P	Si	Cr	Ni	Cu
wt. %	0.95	0.25	S < 0.025	0.15	0.15	0.2	0.2

**2.1 Characterization and Analytical Methods**

The Atomic Force Microscope (AFM) is a technique widely used to provide images of our surface of a échantillon. Elle achieves very high resolution levels up to the atomic level. So we can make surfaces images with very high resolution. When the tip approaches the sample surface (at a distance of a few tenths of a nanometer), forces of Van der Waals repulsion between the atoms of the tip and those of the test surface causes a deflection of the beam depends on the distance that separates them. The main mode of utilization of an AFM microscope is based on the use of a feedback loop to maintain a constant distance between the tip and the surface analyzed using a piezoelectric actuator. Images (3 µm × 3 µm) of the surface of some of our films were obtained using a constant force of 0.035 N/m and determine their respective roughness. It is observed in AFM images Fig. 2 the areal density of the columns decreases with the thickness, which corroborates the fact that the columns are larger. The layers should show a hardness decreases as their thickness increases. Note that the roughness decreases with the column width. The roughness from 44 nm to 3.7 nm for this MoZrN coating, and 73.2 nm to 2 nm for MoN coating (Fig. 3). Indeed, early in the growth of the layer is first create islands that will coalesce and impede the movement of dislocations.

The figure shows the structure of MoZrN and MoN. It appears a particle size of about 80 nm dispersed randomly.

**3. RESULTS AND DISCUSSION**

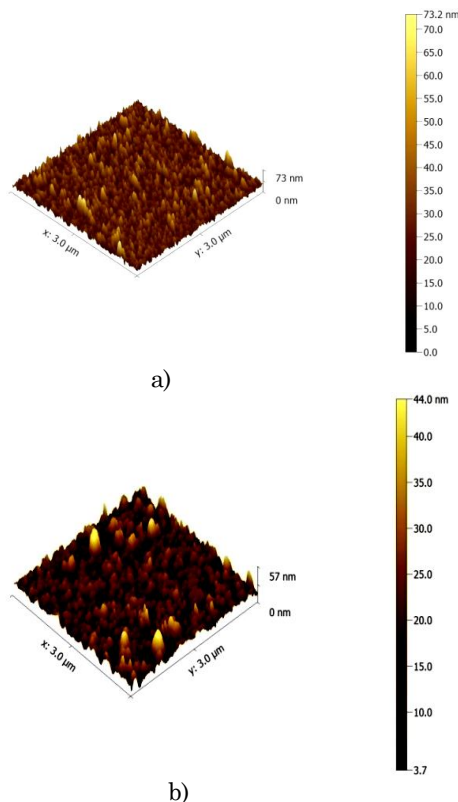


**Fig. 2** – Surface morphologies (AFM) a) Mo-N and b) Mo-Zr-N

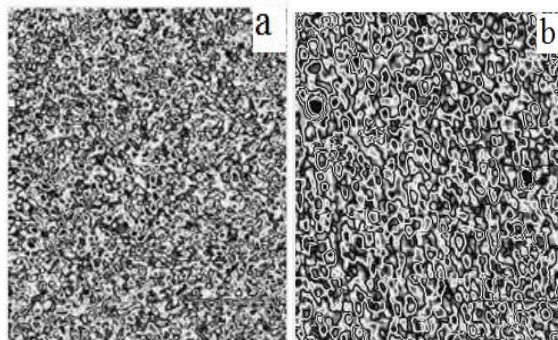


**Fig. 3** – Surface morphologies of a) Mo-N b) Mo-Zr-N

**3.1 Thickness of the films according to the deposition time.**

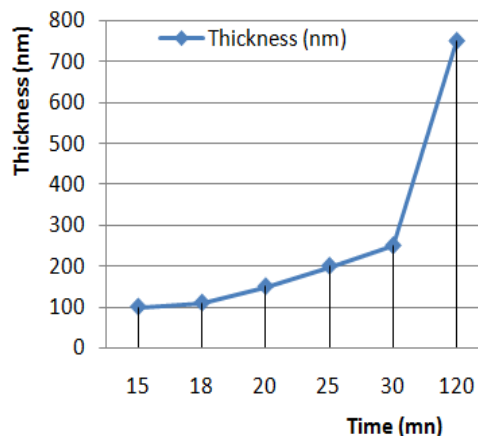


**Fig. 4** – Thickness a function of the time

According to (Fig. 4) we see that the deposited thickness is linearly increasing with deposition time. The speed deposition rate of 6.475 nm/min.

Therefore the deposited mass per surface area of the substrate is also XC100 linear with the deposition.

### 3.2 Residual Stresses as a Function of the Thickness

The compressive residual ( $\sigma$ ) of these coatings stresses are calculated with the formula of Stoney [9].

$$\sigma = \pm \frac{E_s}{6(1-\nu_s)} X \frac{e_s^2}{e_f} \left( \frac{1}{R} - \frac{1}{R_0} \right)$$

where  $\sigma$  is the residual stress in the thin film,  $E_s$  and  $\nu_s$  are Young's modulus (195 GPa) and Poisson's ratio (0.29) of the substrate,  $e_f$  and  $e_s$  indicate the film and substrate thicknesses, respectively,  $R$  is the curvature radius of the sample after deposition,  $R_0$  the curvature radius before deposition.

The decrease of the stress when the thickness increase is attributed to relaxation of the layer in surface. It is noted that the stress of ZrN layers (Fig. 5) is not constant with the thickness. It reaches a maximum and then decreases to 100 nm to 250 nm. Such results have been reported for layers of aluminum nitride [10]. The stress peak is due to a change in structure during growth of the layer

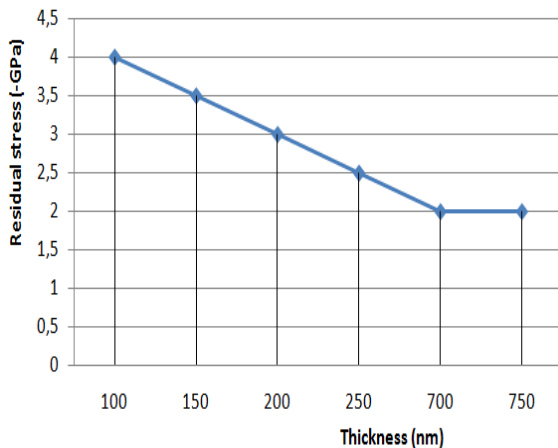


Fig. 5 – Residual stresses as a function of the thickness

### 3.3 Coefficient of Friction as a Function of the Thickness

The friction coefficient of the XC100 steel with the diamond.

The (Fig. 6) represents the coefficient of friction of a film according to ZrN thickness, the friction coefficient of mono and multilayer films on XC100 steel is higher than that of the carbide films. It is between 0.08 and 0.11 and remains very low. Moreover, the layers formed by magnetron sputtering to have a high friction coefficient. Layers of CrN deposited on high speed steel by arc evaporation and to reduce the coefficient of friction was also obtained by Stoney [11].

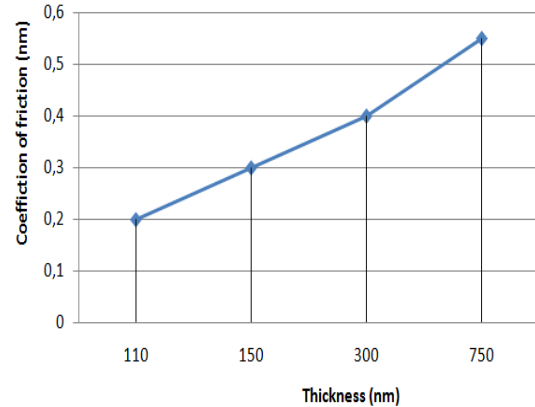


Fig. 6 – Coefficient of friction as a function of the thickness

### 3.4 Variation of the Hardness and the Modul of Young According to the Thickness

The (Fig. 7) Show the effect of the thickness of the coat(layer) on the hardness and the module of Young of the movies of MoZrN. The hardness and the module of Young evolve in the same way as the residual constraints according to the thickness. We observe that for the low(weak) thicknesses, between 0.5 and 0.55  $\mu\text{m}$ , the hardness varies between 15 and 13 GPa and the module of Young between 190 and 160 GPa.

For the thicknesses which exceed (overtake) 2  $\mu\text{m}$ , the values of hardness and module of Young fall(flop) respectively to 6 and 160 GPa. We confirm here that the most thick coats (layers), which seemed according to the observations to the MEB and in the least dense AFM, are the least forced and the least hard.

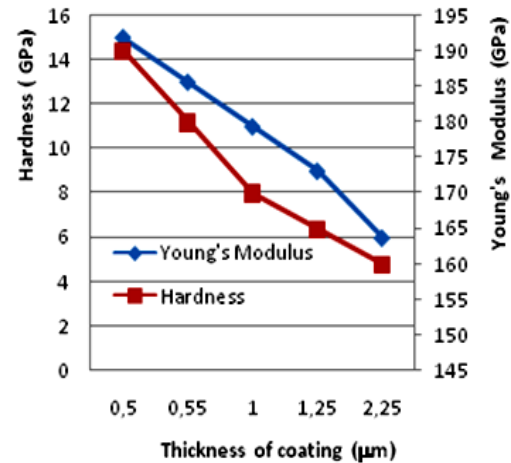


Fig. 7 – Evolution of mechanical properties according to the thicknesses

### 3.5 Deposition Rate as a Function of (% nitrogen)

In the studied range of nitrogen, there is a significant variation in the deposition rate as a function of nitrogen (Fig. 8). It is noted that the deposition rate decreases as the nitrogen increases, the decrease of the deposition rate as a function of nitrogen is due to the increase in the bias voltage of the target when the power applied generator; inducing higher energy bombarding the target species; is increased.

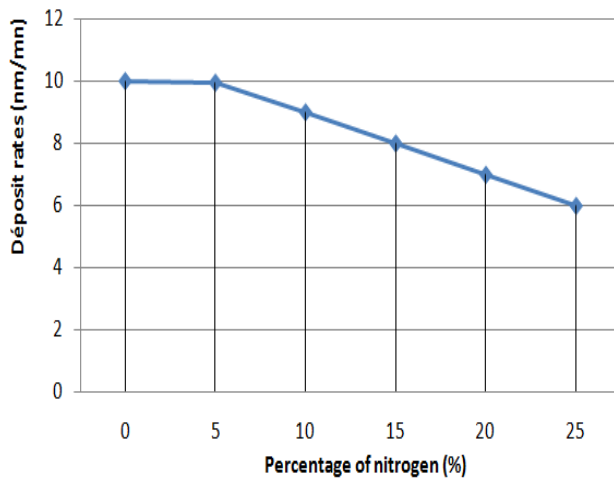


Fig. 8 – Deposition rate as a function of (% nitrogen)

#### 4. CONCLUSION

The present study reflect the influence of various hard coatings on steel XC100.

It appears that the ZrN layer deposited by magnetron sputtering gives better results than the nitriding treatment. Multilayer coatings (MoZrN) and ZrN in all tests resist corrosion. This may be due to a better adhesion of the coating on the substrate and a lower coefficient of friction, which also reduces the cutting forces and the process is more stable with respect to vibration, the thickness of the layer is very significant on the surface.

#### ACKNOWLEDGEMENTS

The authors want to thank especially Pr. Djebaili H. for his advices and collaboration during this work.

#### REFERENCES

1. A. Schulz, H.-R. Stock, P. Mayr, J. Staeves, D. Schmoeckel, *Surf. Coat. Technol.* **94-95**, 446 (1997).
2. A. Hermann, A. Jehn, *Surf. Coat. Technol.* **131**, 433 (2000).
3. H.Y. Lee, J.G. Han, S.H. Baeg, S.E.H. Yang, *Thin Solid Films* **420-421**, 414 (2002).
4. P. Hones, R. Sanjinés, F. Lévy, *Thin Solid Films* **332**, 240 (1998).
5. R.J. Rodríguez, J.A. García, A. Medrano, M. Rico, R. Sánchez, R. Martínez, C.D. Sangiovanni, L. Hultman, V. Hirita, *Acta Materialia* (2011).
6. J. Richter, *Surf. Coat. Technol.* **162**, 119 (2003).
7. K. Kutschej, B. Rashkova, J. Shen, D. Edwards, C. Mitterer, G. Dehm, *Thin Solid Films* **516**, 369 (2007).
8. G.G. Stoney, *Proc. Royal. Soc. A*, **82**, 172 (1909).
9. W. Kutschej, *7<sup>ème</sup> Symposium International sur les Tendances et Applications des Films Minces TAFT* (Nancy: France: 2000).
10. S. Lee, F. Lai, *Mater. Chem. Phys.* **43**, 266 (2000).
11. P. Panjan, B. Navinšek, A. Cvelbar, A. Zalar, I. Milošev, *Thin Solid Films* **281**, 298 (1996).